Anal Bioanal Chem (2014) 406:5645–5656
DOI 10.1007/s00216-014-7971-9

RESEARCH PAPER

Multiwell cartridge with integrated array of amorphous silicon photosensors for chemiluminescence detection: development, characterization and comparison with cooled-CCD luminograph

Mara Mirasoli · Augusto Nascetti · Domenico Caputo · Martina Zangheri · Riccardo Scipinotti · Luca Cevenini · Giampiero de Cesare · Aldo Roda

Received: 31 March 2014 / Revised: 26 May 2014 / Accepted: 12 June 2014 / Published online: 26 June 2014

Abstract We propose a disposable multiwell microcartridge with integrated amorphous silicon photosensors array for bio- and chemiluminescence-based bioassays, where the enzymatic reactions and the detection unit are coupled on the same glass substrate. Each well, made in a polydimethylsiloxane (PDMS) unit, hosts an enzymatic reaction that is monitored by one photosensor of the array. Photosensors were characterized in terms of their dark current background noise and response to different wavelengths of visible light in order to determine their suitability as detection devices for chemical luminescent phenomena. Calibration curves of the photosensors' response to different luminescent systems were then evaluated by using the chemiluminescent reactions catalyzed by alkaline phosphatase and horseradish peroxidase and the bioluminescent reaction catalyzed by firefly luciferase. Limits of detection in the order of attomoles for chemiluminescence enzymes and femtomoles for luciferase and sensitivities in the range between 0.007 and 0.1 pA $pmol^{-1}$ L were reached. We found that, without the need of cooling systems, the analytical performances of the proposed cartridge are comparable with those achievable with state-of-the-art thermoelectrically cooled charge-coupled device-based laboratory instrumentation. In addition, thanks to the small amount of generated output data, the proposed device allows the monitoring of long-lasting reactions with significant advantages in terms of data-storage needs, transmission bandwidth, ease of real-time signal processing and limited power consumption. Based on these results, the operation in model bioanalytical assays exploiting luminescent reactions was tested demonstrating that a-Si:H photosensors arrays, when integrated with PDMS microfluidic units, provide compact, sensitive and potentially low-cost microdevices for chemiluminescence and bioluminescence-based bioassays with a wide range of possible applications for in-field and point-of-care bio-analyses.

Keywords Chemiluminescence · Bioluminescence · Amorphous silicon photosensors · Integrated analytical systems · Point of care · Lab-on-chip

Mara Mirasoli and Augusto Nascetti contributed equally to the work.

Published in the topical collection *Analytical Bioluminescence and Chemiluminescence* with guest editors Elisa Michelini and Mara Mirasoli.

M. Mirasoli (✉) · M. Zangheri · L. Cevenini · A. Roda
Department of Chemistry "G. Ciamician,", University of Bologna, 40126 Bologna, Italy
e-mail: mara.mirasoli@unibo.it

M. Mirasoli · L. Cevenini · A. Roda
National Institute of Biostructure and Biosystems (INBB), Interuniversity Consortium, 00136 Rome, Italy

A. Nascetti (✉)
Department of Astronautical, Electrical and Energy Engineering, Sapienza University of Rome, 00138 Rome, Italy
e-mail: augusto.nascetti@uniroma1.it

D. Caputo · R. Scipinotti · G. de Cesare
Department of Information, Electronics and Communication Engineering, Sapienza University of Rome, 00184 Rome, Italy

Introduction

Recent progresses in the fields of life sciences and microtechnology have led to the development of lab-on-chip (LOC) devices that can perform analysis of small amounts of sample, employing portable and miniaturized analytical instrumentation [1]. However, only few LOC are currently commercially available and in many cases laboratory equipment is still required for their operation. Thus, current research efforts are directed towards the integration of all the necessary

components into a single analysis tool in order to produce a true LOC system [2–5].

Among optical detection techniques employed in LOC devices, bioluminescence (BL) and chemiluminescence (CL), based on the production of photons as a result of a chemical reaction, are particularly advantageous for the development of ultrasensitive analytical systems in miniaturized formats, offering high detectability even in small volumes (due to the very low background) and large dynamic range of the signal [6–9]. In addition, as the chemical reaction acts as an internal light source, the equipment required for signal acquisition is rather simple, with no necessity for excitation light sources, focusing optics, wavelengths selectors, and specific design of the measurement cell [10, 11]. These features significantly reduce background emission from interfering compounds or device components usually encountered in fluorescence-based assays, as well as power consumption. However, BL and CL usually involve the emission of low light levels, thus requiring highly sensitive detectors, such as cooled CCDs or photomultiplier tubes [12] and in most cases integrated detectors did not offer satisfactory detectability.

We have recently reported a device based on a cooled charge-coupled-device (CCD) exploiting a lensless contact-imaging approach. With this system, coupled with a microfluidic module, it was possible to perform multiplex BL and CL bioanalytical assays reaching detectability levels comparable with those obtained with reference laboratory instrumentation [13–15]. However, although the device was compact and portable, full integration of the detector and reduction of power consumption are required to obtain a true LOC system, still maintaining the same analytical performance.

One of the most promising materials to this aim is amorphous silicon (a-Si:H) and its alloys. The low deposition temperature (<250 °C), that is compatible with a wide range of support materials, and the use of microelectronics technologies for the fabrication of sensor arrays make a-Si:H a good candidate for application in microfluidic devices [16], where simultaneous detection of different parallel reactions is needed. In addition, the a-Si:H physical characteristics prompt the use of this material in different devices, such as solar cells [17], electronic switching [18], physical [19] and optical sensors. In particular, a-Si:H photosensors are characterized by very low dark currents and a high quantum efficiency in the wavelength range from ultraviolet [20] to near infrared [21, 22]. The use of thin-film a-Si:H photosensors for the detection of biomolecules has been already reported by different research groups [23], for measuring the optical absorbance in the UV range [24], fluorescence [25, 26], or CL signals [27–30].

In this work, in order to state the suitability of a-Si:H photodiodes as ultrasensitive detection devices for LOC systems, we designed, fabricated and characterized a LOC system with integrated photosensors and applied it to two different "model" bioassays. The system includes an array of 16 a-Si:H photodiodes deposited on a glass substrate, on which a PDMS unit containing 16 wells was applied to obtain an integrated microcartridge. A custom portable readout electronic board was employed. This device, in which the luminescent signal is generated and measured in close proximity, provides efficient photon transfer between the sample-well and the photosensors, as well as very compact dimensions, favorable for miniaturization.

Firstly, device performances were characterized at the photosensor level and at analytical level in terms of noise, sensitivity, detectability with different CL and BL systems, comparing the analytical performances with reference state-of-the-art laboratory instrumentation. Finally, the device functionality was successfully tested on two model bioanalytical BL (cell toxicity assay) and CL (total antioxidant capacity measurements) assays.

Materials and methods

Reagents

The enzymes horseradish peroxidase (HRP) type VI-A and alkaline phosphatase (ALP) from bovine intestinal mucosa, as well as activated charcoal and ascorbic acid were purchased from Sigma-Aldrich (St. Louis, MO). Firefly luciferase (Luc) stock solution (5 mg mL^{-1}) was from the ATP Determination Kit (Molecular Probes). The Super Signal ELISA Femto CL cocktail for HRP was purchased from Thermo Fisher Scientific (Rockford, IL), while the Lumiphos Plus CL cocktail for ALP was from Lumigen (Southfield, MI). The BL cocktail for Luc measurements was Britelite plus (PerkinElmer Inc., Waltham, MA).

Polydimethylsiloxane (PDMS) Silgard 184 pre-polymer and curing agent were from Dow Corning (Midland, MI).

All solutions were prepared in 0.1 M phosphate buffered saline (PBS) pH 7.7 employing Milli-Q Plus ultra-pure water.

Materials for photolithography process (photoresist AZ-1518, developer AZ351B remover AZ100 and etchants for metals) were purchased from Sigma-Aldrich, while SU-8 2005 photoresist, its developer and its remover were purchased from Micro Resist Technology GmbH (Germany). In all the microelectronic processes, water for last rinsing was purified with a Milli-Q Plus (Millipore, R=18.2 MΩ·cm) ultra-pure water system.

Instrumentation

The Night Owl LB 981 (Berthold Technologies, Bad Wildbad, Germany) was employed as a reference instrumentation. The system is equipped with a 512×512-pixel back-

illuminated slow-scan CCD sensor, thermoelectrically cooled to −50 °C to reduce the background noise. The Winlight 1.2 (Berthold Technologies) software was used for image acquisition and processing. All images were acquired employing a 4-s integration time.

Chemiluminescence and bioluminescence spectra were recorded using a Varian Eclipse spectrofluorimeter (Varian Inc., Palo Alto, CA).

Photosensor array fabrication

The photosensors are p-doped/intrinsic/n-type stacked structure deposited on a glass substrate covered with an indium tin oxide (ITO) layer that acts both as transparent window layer for the BL and CL signal and as electrical bottom contact for the a-Si:H diodes. Metal films deposited on the a-Si:H layers behave both as photosensor top electrode and electrical contact lines. Amorphous silicon layers were deposited by a three UHV chambers plasma- enhanced chemical vapor deposition (PECVD) system (from Glasstech Solar Inc.), metal films were deposited by a BALZERS 510 vacuum evaporation system while ITO layer was grown by a magnetron sputtering system from Materials Research Corporation (Orangeburg, NY, USA).

The fabrication of the photosensor array was performed through the following steps:

1. Deposition of 150-nm-thick ITO by magnetron sputtering and its pattering by wet etching (solution of H_2O_2:HCl= 1:3) for definition of the bottom electrode;
2. Deposition by PECVD of the three a-Si:H layers. The deposited thicknesses were 10, 400 and 50 nm for the p-type, intrinsic and n-type material, respectively;
3. Deposition by magnetron sputtering of a three metal layer stack (30 nm-thick Cr/150 nm-thick Al/30 nm-thick Cr) acting as back electrode of the sensors;
4. Mesa patterning of the device structure by wet and reactive ion etching for the metal stack and a-Si:H layers respectively (the area of each photodiode is 2×2 mm^2);
5. Deposition of a 5 μm-thick SU-8 layer acting as insulation layer between the back metal and the front TCO contacts;
6. Opening of via holes over the diodes on the passivation layer;
7. Sputtering of a 100 nm-thick TiW metal layer over the passivation layer;
8. Patterning of the TiW external contacts for the definition of the back contact and the external connection of the photodiodes.

The photolithographic processes were performed using a TAMARACK 152R mask-aligner for mask reproduction, a Reactive Ion Etching system (from IONVAC PROCESS, Italy) for dry etching of amorphous silicon films and a chemical bench for wet etching of metal films. All the microelectronic processes have been performed in a clean room.

After fabrication, the photodiodes have been individually tested to evaluate their electrical and electro-optical characteristics. The photosensor current-voltage characteristics were evaluated using a Keithley 236 Source Measure Unit (SMU), while the sensor responsivity was measured by using a quantum efficiency setup, which includes a tungsten light source, a monochromator (model Spex 340E from Jobin-Yvon), a UV-enhanced crystalline silicon diode (model DR 2550-2BNC from Hamamatsu) used as reference, a beam-splitter and focusing optics (from Melles-Griot).

For the characterization of the sensor array as a whole and for the subsequent experimental part, portable custom readout electronics has been used for the simultaneous measurement of the current of the 16 photodiodes [31]. The a-Si:H photosensor array was connected to the custom readout electronic board using a flex connector. The low-noise readout electronics is based on eight ACF2101 dual-channel charge sensitive preamplifiers from Texas Instruments that integrate the sensor current providing a proportional output voltage that is converted to digital by a MAX180 12-bit analog to digital converter from Maxim. The sensor bias is sourced by a 12-bit digital to analog converter whose output has been buffered with a AD8510 operational amplifier to ensure correct driving of the large capacitive load represented by the 16 photodiodes in parallel. The entire front-end board is controlled by a TUSB3210 microcontroller that also provides the USB link to an external computer where a graphical user interface allows to easily operate the entire system from acquisition setup to data storage.

Microwell cartridges fabrication

Disposable 16-well cartridges with integrated photosensors were obtained by coupling a 10-mm-thick black PDMS unit comprising an array of 16 through holes with the glass support where the 16-photosensor array had been deposited.

Pre-polymer and curing agent were mixed at a 10:1 ratio (*w*/*w*) and activated charcoal (3 %, *w*/*w*) was added to obtain black PDMS mixture, which was vacuum treated for 15 min to remove air bubbles, then cast in a mold containing 16 pillars (2×2 mm) in positions corresponding to the photosensors in the array. After 16 h of polymerization at room temperature, the structured PDMS was peeled off from the mold and coupled with the glass substrate aligning the wells with photosensors and exploiting the sticky nature of partially cured PDMS, as previously reported [29].

Chemiluminescence measurements

The chip of photosensors was placed inside the CCD-based Night Owl LB 981 luminograph light-shielded box to ensure

dark conditions during the experiments and to acquire luminescent signals simultaneously with the two instruments. A picture of the measurement setup is reported in Fig. 1.

The ability of photosensors to provide quantitative measurement of the emitted photons down to low light levels was evaluated by deriving the calibration curve in a concentration range significant for each specific enzyme.

At the beginning of each experiment, the background signal was measured for both detection systems in absence of luminescent solutions. For each measurement 2 μL of enzyme solution (HRP, ALP, or Luc) at different concentrations (buffer for the blank) and 8 μL of the respective luminescent cocktail were dispensed in the wells. The measurements of the luminescence signals were performed with a delay of 20 s after the closure of the dark box, to ensure that the signal measured by the photosensors was not altered by a memory effect due to exposure to ambient light [32]. The luminescent signal was monitored with the a-Si:H photosensors and the CCD simultaneously, through consecutive acquisitions of the same integration time to enable a comparison of analytical performance of the two devices. In particular, the integration time used for each acquisition was 3.98 s for the photosensors (thus enabling a measurement of photocurrent every 4 s) and 4 s for images acquired with the CCD. The CCD frame rate was one image every 15 s, as a trade-off between time resolution of process monitoring and data-storage requirements.

Each point of the calibration curve corresponds to the plateau value of photocurrent measured during the entire luminescent reaction kinetics averaged over three independent measurements.

The reported limits of detection (LOD) have been calculated as the enzyme concentration whose signal corresponds to three times the standard deviation of the blank signal, which is the signal measured when the CL cocktail was poured in a well without the enzyme. Such standard deviation accounts for electronic noise, photodiodes shot noise, as well as the variation of the low autoluminescence of the CL cocktail.

Cytotoxicity test

A volume of 100 μL of human embryonic kidney cells (HEK293) genetically modified to stably express Luc (6,000 cells suspended in liquid culture medium) was incubated with 100 μL of dimethyl sulfoxide (DMSO) at different concentrations (in the range 2–50 %, *v*/*v* in culture medium, only culture medium for the blank) for 90 min at 37 °C. Then, 20 μL of the mixture were transferred in the PDMS cartridge wells and, upon addition of 20 μL of BL cocktail, photons emission was acquired as reported above (4 s consecutive acquisitions for a total of 10 min).

Total antioxidant activity measurements

Ten microliters of ascorbic acid solutions (between 0 and 50 μM, only buffer for the blank) was dispensed into each well of the PDMS microcartridge in duplicate, then 20 μL of Super Signal ELISA Femto CL cocktail containing the enzyme HRP (4 pg μL^{-1}) was added. In parallel, 10 μL of two red grape must extract samples (one ethanol extract and one aqueous extract) were assayed in triplicate, upon dilution with water (1:500 and 1:100, *v*/*v*, respectively). Photons emissions were acquired at 4-s frame rate for a total of 10 min in order to assess the kinetics of CL emission.

Results and discussion

Integration of all the key elements in a single miniaturized analytical device is currently one of the main issues to be solved for the realization of true and effective micro total analysis systems (μTAS). Among optical detection principles, CL offers low detection limits in small volumes and rapidity and it is thus particularly suited for LOC applications [33–37]. Due to the small volumes employed in miniaturized analytical devices and to the low light emission inherent in all BL and

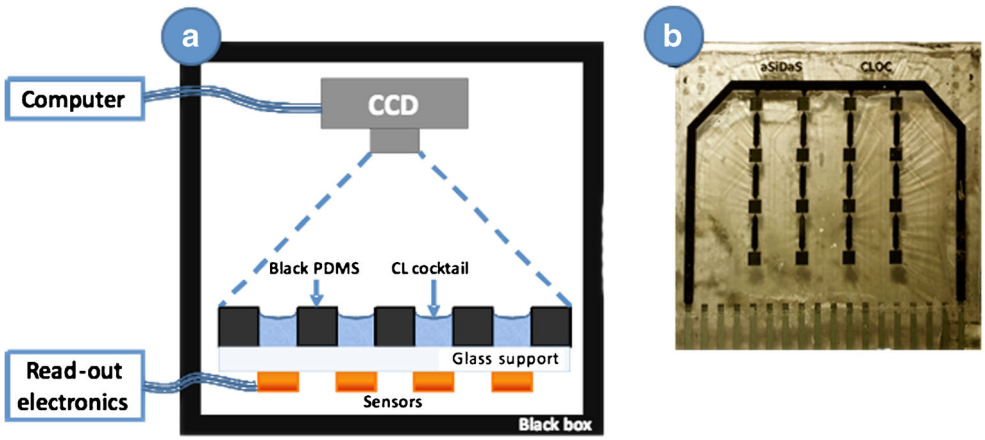

Fig. 1 Experimental setup: **a** schematic overview of the 16-well microcartridge with integrated a-Si:H photosensors positioned in the CCD-based luminograph. **b** Close view of the photosensors array

CL reactions, highly sensitive radiation detectors must be employed, along with configurations ensuring high collection efficiency of photons. In addition, to ensure multiplex capability, either imaging devices or photosensors arrays are required.

In this work, we propose disposable microcartridges for BL and CL-based bioassays integrating arrayed a-Si:H photosensors. To enable out-of-laboratory applications, custom portable readout electronics has been used for the simultaneous measurement of the currents of the 16 photodiodes. Sensors architecture and custom readout electronics design have been optimized to reach the required detectability and to ensure adequate reproducibility of response between sensors in the array. The arrayed a-Si:H photosensors were coupled with a PDMS unit to obtain disposable cartridges containing 16 black wells with clear bottom (40 μL each) in which chemical reactions are performed in close proximity to the sensors, fabricated on the opposite glass substrate side to avoid issues of chemical compatibility.

Each photodiode has been first tested regarding its electrical and electro-optical characteristics. Then, the analytical performance of the arrayed a-Si:H photosensors in the measurement of BL and CL emissions was evaluated, as compared with reference cooled slow-scan CCD-based imaging instrumentation. Finally, their ability to provide real-time measurement of evolving BL and CL reactions was exploited for performing model luminescent bioassays, namely a BL-based cytotoxicity assay and a CL enzyme-based assay for total antioxidant capacity measurement.

Photosensor characterization

The a-Si:H photosensors were characterized by measuring both the current-voltage (I-V) curve in dark condition and the spectral response in the visible range (Fig. 2). These measurements allow to determine the dark current noise in the operation condition and the sensor sensitivity at the different wavelengths.

Figure 2a reports the average I-V characteristics of three different diodes of the array, measured in dark conditions. The photodiodes characteristics are quite uniform all over the array with a value of the dark current in the order of 10^{-10} A cm^{-2} in reverse bias conditions. Taking into account that the measurements have been taken with a signal bandwidth of 1 Hz and that the photosensor area is 4 mm^2, the root-mean-squared (rms) dark current noise was calculated to be around 1.6 fA. This value is below the experimental noise introduced by the experimental characterization setup, which is around 10 fA.

Quantum efficiency curves averaged over three different photosensors of the array are reported in Fig. 2b. Again, a good uniformity of response over the array can be inferred. The thickness and doping of the different a-Si:H layers have been designed in order to achieve a wide spectral response, that enables the use of different BL and CL reactions with the same device, exploiting the advantages of chemical luminescence over photoluminescence, where the need of the filtering of the excitation light impacts on the design of the photosensor structure and assay sensitivity. The normalized emission spectra of the three luminescent reactions considered in this work are also reported in Fig. 2b for comparison. The luminol/peroxide/enhancer CL reaction catalyzed by HRP has a maximum emission at 425 nm, while the CL reaction catalyzed by ALP in the presence of Lumiphos Plus cocktail displays a maximum emission at 470 nm. The firefly Luc-luciferin ATP Mg^{2+} BL reaction has a maximum emission at 565 nm. All the considered luminescence emission spectra, spanning from violet-blue to yellow-greenish light, match reasonably well with the response of the photodiodes. It is worth noting that

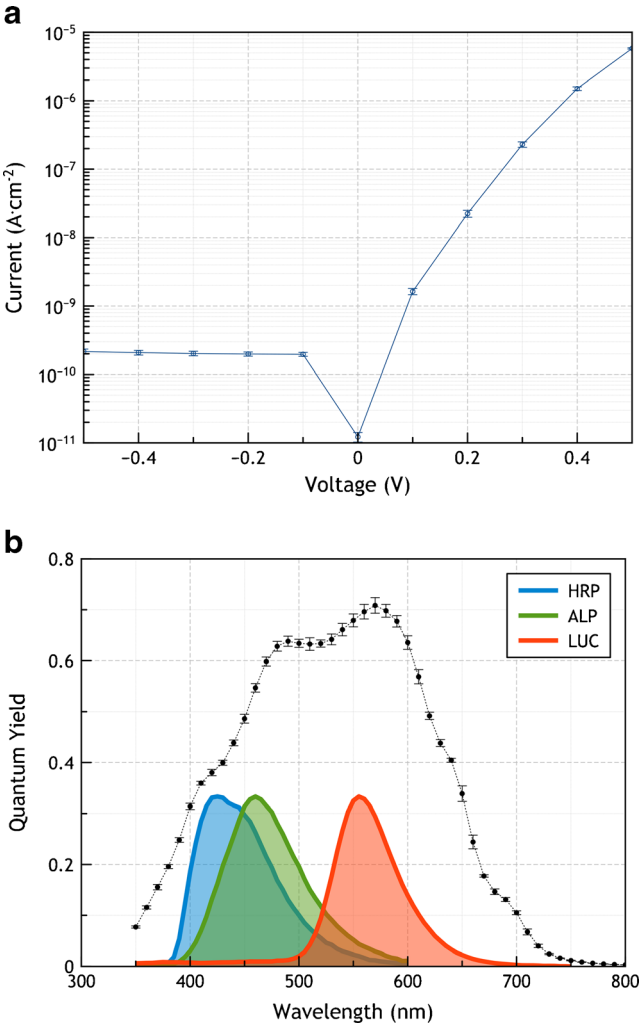

Fig. 2 Characteristics measured for three diodes of the a-Si:H array: **a** current-voltage curves; **b** normalized quantum efficiency curve. The maximum of the quantum efficiency curve, occurring at 580 nm, is equal to 0.72. In the same graph, the emission spectra of the luminescent reactions studied in this work are shown: each spectrum is normalized to its maximum emission value

spectral response can be differently tuned for other specific wavelengths of interest by proper sensor design, thus possibly extending applications also to red-shifted BL and CL reactions.

According to the QY curve, the photosensor responsivity at the emission wavelength of the investigated molecules can be derived. Starting from the definition of the responsivity (R) as:

$$R(\lambda) = \mathrm{QY}(\lambda) \cdot \lambda \Big/ 1,240(\mathrm{nm})$$

we infer that the photosensor responsivity is equal to 140, 235 and 320 mA W^{-1} for the luminescent reactions catalyzed by HRP, ALP and Luc, respectively.

It is worth now to compare the main characteristics of our photosensor with other optical detectors integrated in microfluidic chip. Table 1 reports the responsivity, dark level, size and noise level of devices based on both organic and inorganic materials.

We can observe that the performances of our photosensor are within those of the other proposed systems. Our device shows a lower responsivity at 425 nm with respect to that reported by Pereira et al. [38], but it presents lower dark current and better noise performances. The very high responsivity showed by the graphene-based photosensor, due to its internal gain, is counter-balanced by a much higher dark current, higher thermal budget and more complex fabrication process [39]. Photodetectors based on organic materials present good performances in terms of both responsivity and dark current levels, even though their fabrication and technology processes are not completely assessed [40, 41].

Results presented in more details in the next sections will show that the characteristics of the proposed system make it suitable for lab-on-chip analysis requirements, since its analytical performances are very close to that of cooled back-illuminated CCD-based reference instrumentation.

Bio- and chemiluminescence measurements

Chemical luminescent measurements were performed by using three luminescent systems that are widely used in bioanalytical applications, namely, CL reactions catalyzed by HRP or ALP enzymes (widely used in enzyme-based assays and binding assays as gene probe hybridization and immunoassays), and the BL reaction catalyzed by firefly Luc (employed as a reporter gene in recombinant cell-based biosensors). Results are summarized in Table 2. In chemical luminescence reactions, light detected is a transient product of the reaction that is only present while the enzyme- enzymatic substrate reaction is occurring. When the enzyme is employed as a label, the enzymatic substrate is added in excess to obtain light emission proportional to enzyme amount.

Calibration curves were obtained for each enzyme, measuring light emission in parallel with the a-Si:H photosensors and the CCD-based luminograph. It has to be pointed out that the CCD sensor was thermoelectrically cooled down to −10 °C, which decreases the background signal (both in terms of absolute value and instrumental noise) due to the thermal generation of electrons, while the a-Si:H photosensors were employed at room temperature (about 25 °C) in view of their use in a on-the-field application as well as to avoid cooling down of biological reactions that occur on the opposite side of the same glass substrate, which would largely affect their kinetics.

Table 1 Characteristics of the reported a-Si:H photosensors, as compared with the reference CCD-based luminograph and with other recently reported devices based on both organic and inorganic materials

Device	Responsivity	Dark level	Sensor size	Noise level
a-Si:H photosensor [38]	200 mA W^{-1} (λ=425 nm)	10^{-9} A cm^{-2}	200×200 μm^2	$2 \cdot 10^{-10}$ A cm^{-2} (due to the luminescent measurement)
Graphene phototransistor [39]	Up to 10^3 A W^{-1} @ λ=532 nm (depends on the light intensity and applied voltage)	Up to 200 mA @ −40 V	80 μm^2	10^{-8} A $Hz^{-1/2}$ @ 1Hz modulation frequency
Organic photodetector (made in P3HT:PCBM) [40]	200 mA W^{-1} @ 550 nm (very low below 450 nm)	0.59 μA cm^{-2}	1 mm^2	–
Polymer photodiode (made in PCDTBT: PC70BM and PEDOT:PSS) [41]	~250 mA W^{-1} (in the range 425–500 nm)	2 pA	4×4 mm^2	–
CCD-based Night Owl LB 981 (Berthold Technologies, Bad Wildbad, Germany)	242 mA W^{-1} (λ=425 nm) 258 mA W^{-1} (λ=470 nm) 274 mA W^{-1} (λ=565 nm)	≤5 10^{-4} e^- $pixel^{-1}$ s^{-1}		7 e^- RMS
Our device (a-Si:H photosensor)	140 mA W^{-1} (λ=425 nm) 235 mA W^{-1} (λ=470 nm) 320 mA W^{-1} (λ=565 nm)	10^{-10} A cm^{-2}	2×2 mm^2	250 fA cm^{-2}

Table 2 Parameters of the calibration curves obtained for the three assayed luminescent reactions and the two types of detection systems employed

	a-Si:H photosensors array	CCD-based luminograph
Alkaline phosphatase		
R^2 value	0.998	0.997
Sensitivity	0.012 pA $pmol^{-1}$ L	29 RLU $pmol^{-1}$ L
Limit of detection	30 pmol L^{-1}	19 pmol L^{-1}
Firefly luciferase		
R^2 value	0.999	0.998
Sensitivity	0.0067 pA $pmol^{-1}$ L	30 RLU $pmol^{-1}$ L
Limit of detection	500 pmol L^{-1}	160 pmol L^{-1}
Horseradish peroxidase		
R^2 value	0.989	0.999
Sensitivity	0.45 pA $pmol^{-1}$ L	1300 RLU $pmol^{-1}$ L
Limit of detection	1.6 pmol L^{-1}	0.7 pmol L^{-1}

Alkaline phosphatase

Calf intestinal ALP is a 160 kDa enzyme often employed as a marker for CL assays employing 1,2-dioxetane derivatives as enzymatic substrates. In this work, a CL cocktail for ALP containing 4-methoxy-4-(3-phosphatephenyl)spiro [1,2-dioxetane-3,2′-adamantane] disodium salt (AMPPD) and an enhancer (which increases the duration and intensity of the emission) was employed. The catalytic action of the enzyme on AMPPD results in dephosphorylation of the aryl phosphate moiety of the dioxetane with subsequent cleavage of the 1,2-dioxetane ring, production of a phenolate moiety in its excited state, and photons emission [42].

A typical curve of the kinetics of photon emission measured with on-chip a-Si:H photosensors is reported in Fig. 3, in which 2 μL of a 3×10^{-4} mg mL^{-1} ALP solution (corresponding to 2 fmol of deposited enzyme), and 8 μL of Lumiphos plus CL cocktail were mixed.

The figure reports the sensor photocurrent calculated from the total measured current by subtracting the dark current value measured before adding the enzyme, which was stable for more than 10 min (CV 0.7 %). The dark current level was around 8 pA for all the photodiodes of the array: this baseline value also accounts for the very weak spontaneous light emission of the CL cocktail in the absence of enzyme. The variance of the baseline signal corresponds to the practical noise of the system, mainly due to the intrinsic photodiode current shot noise, the preamplifier noise and the switching (kTC) noise contributions. Upon enzyme addition, the photocurrent response rapidly increased during the first 5 min and then remained at plateau for at least 5 min (10.8±0.1 pA, inset in Fig. 3) finally decreasing very slowly to the baseline level in approximately 2 h, due to the consumption of CL reagents and/or inactivation of the enzyme. The observed behavior, which was confirmed by the reference CCD system, reflects the typical kinetics of the CL reaction of 1,2-dioxetane compounds catalyzed by ALP [43].

Results show that the a-Si:H photosensors rapidly respond to changes in the CL signal and return to dark signal levels upon completion of the reaction, without any memory effect, thus enabling real-time detection of evolving CL reactions. In addition, the amount of data corresponding to the entire kinetic curve reported in Fig. 3, with 4-s time resolution, occupies about 64 kB of memory, while the 480 raw images, acquired by the CCD camera every 15 s, occupy at least 235 MB (495 kB for each frame). This has a significant impact not only on the data-storage and data-transmission bandwidth, but also on the algorithm complexity and computing time for data analysis.

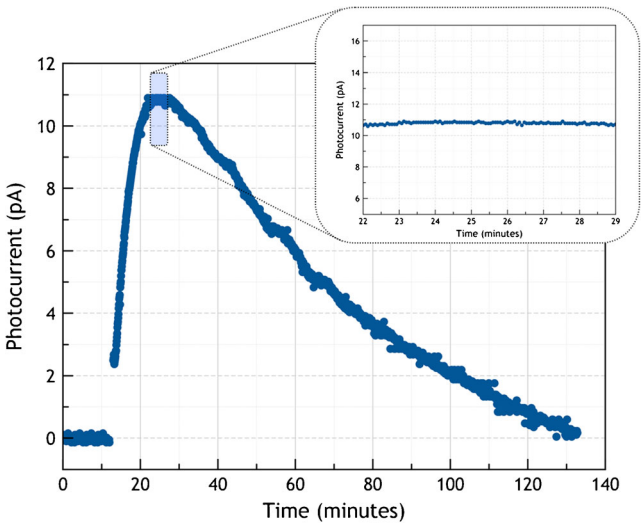

Fig. 3 Kinetics of photon emission of ALP CL system measured with on-chip a-Si:H photodiodes

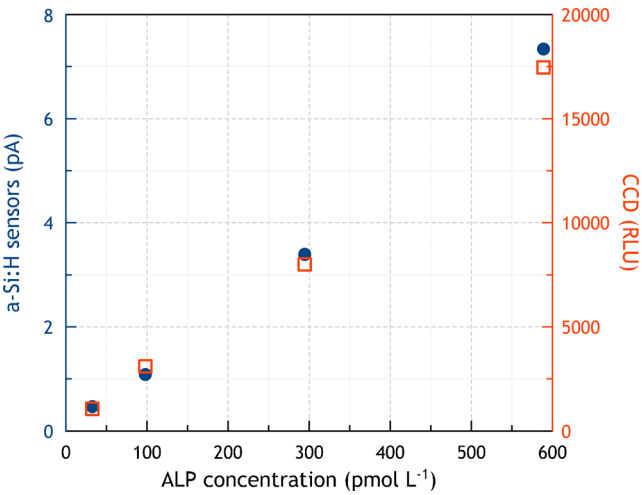

Fig. 4 Calibration curve for ALP employing the Lumiphos Plus CL cocktail. *Circles and squares* refer to the measurements achieved with a-Si:H photosensors and CCD camera, respectively

Calibration curves obtained for the enzyme ALP (in the range between 5 and 100 pg μL^{-1}) employing the 1,2-dioxetane-based CL cocktail are reported in Fig. 4. Circles and squares refer to the data measured with the a-Si:H photosensors and with the CCD-based detector, respectively. Each point referring to the specific ALP concentration is the maximum of the kinetic curve with respect to the signal baseline, averaged over three different experiments. Both curves present an excellent linearity in the investigated range of concentration.

From Fig. 4, the measured sensitivity of the a-Si:H photodiodes is 38.5 fA pg^{-1}. The calculated LOD at three sigma is 5 pg μL^{-1} (corresponding to 65 amol of deposited enzyme), taking into account that the measured standard deviation of the blank signal is 120 fA. Comparison with the LOD of 2.8 pg μL^{-1} obtained employing the CCD demonstrates equivalent performances with state-of-the-art laboratory instrumentation.

Luciferase

Firefly Luc is one of the most widely used reporter proteins for the study of gene expression and for reporter gene-based whole-cell biosensors. Wildtype *Photinus pyralis* luciferase is a 62-kDa protein that in the presence of Mg^{2+}, ATP and molecular oxygen oxidizes its enzymatic substrate, firefly luciferin, emitting yellow-green light (emission maximum ~560 nm). At this wavelength the quantum efficiency of the a-Si:H photosensors is maximum, around 0.72, as shown in Fig. 2b.

Calibration curves were obtained for Luc (in the range between 20 pg μL^{-1} and 2 ng μL^{-1}) employing the luciferin/ATP-based BL cocktail (Fig. 5). A LOD of 30 pg μL^{-1} was calculated (corresponding to 1 fmol of deposited enzyme), while 10 pg μL^{-1} was the LOD obtained with the CCD-based detection.

This is the first report about the measurement of Luc signals with integrated a-Si:H photosensors, which extends possible applications to BL-based assays, such as recombinant whole-cell biosensors for environmental or life science applications.

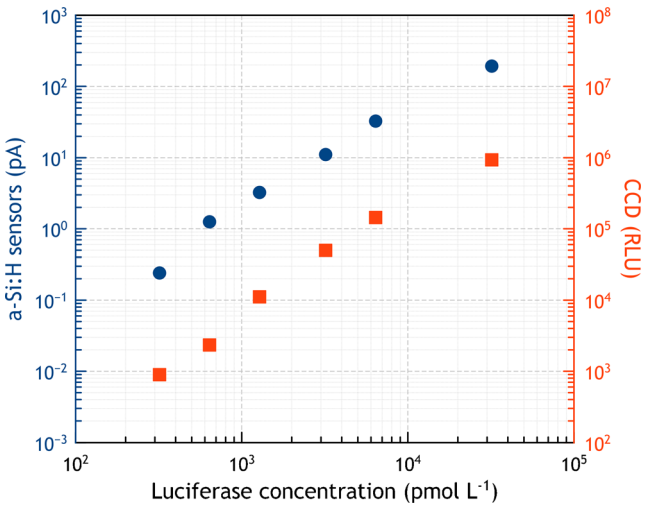

Fig. 5 Calibration curve for Luc employing the Britelite plus BL cocktail. *Circles and squares* refer to the measurements achieved with a-Si:H photosensors and CCD camera, respectively

Horseradish peroxidase

Horseradish peroxidase, which is largely employed in bioanalytical assays owing to its rather low dimension (44 kDa) and high turnover rate, catalyzes the reaction between a hydrogen acceptor (such as hydrogen peroxide) and a hydrogen donor, namely luminol in CL systems. Luminol is oxidized to produce 3-aminophthalate in its excited state, which decays to a lower energy state by releasing photons with maximum emission at 425 nm. The addition of enhancers (such as substituted phenols, substituted arylboronic acid derivatives and other molecules) increases the enzyme turnover number and the equilibrium concentration of the key intermediate luminol radical anion, providing more intense, prolonged and stable light emission [44, 45].

Figure 6 reports the calibration curves, each as the average of three independent measurements, obtained for the enzyme HRP (between 0.025 and 50 pg μL^{-1}) via CCD camera and photosensors. The signal shows in all cases a good correlation with the amount of enzyme present. In particular, by comparing two calibration curves (solid and open circles) obtained employing different a-Si:H photosensor chips produced in different sessions, very high inter-chip reproducibility can be observed. In addition, the calibration curves

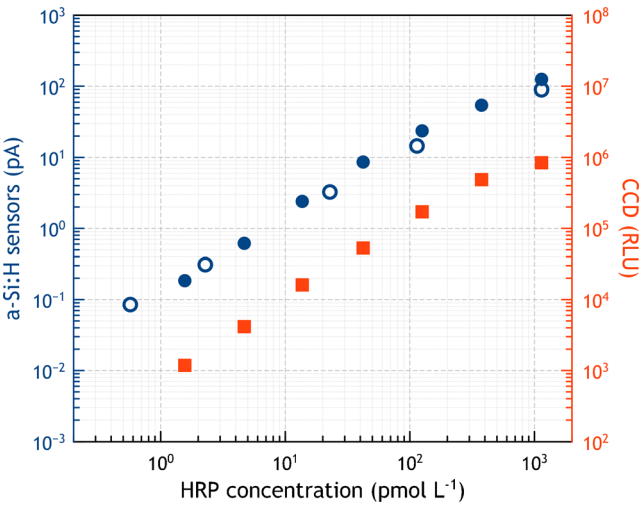

Fig. 6 Calibration curve for HRP employing the SuperSignal ELISA Femto CL cocktail. *Open and solid circles* refer to the measurements achieved with a-Si:H photosensors produced in two different fabrication runs and acquired with the Keithley 236 SMU and with the custom readout electronics, respectively. *Squares* refer to the measurements achieved with the CCD camera

obtained employing the photosensors are consistent with CCD results. Limits of detection were found to be 70 fg μL^{-1} (corresponding to 3 amol of deposited enzyme) for the photosensors, which was only 2.3 times higher than the LOD obtained for the CCD measurement in the same experimental conditions and consistent with previously reported LOD values [43]. The linear response extends up to 5 pg μL^{-1}. Although a slight deviation from linearity is observed at higher concentrations, due to the fact that the CL reagents are not in sufficient excess with respect to enzyme amount as previously reported [29], the dynamic range of the curve covers three orders of magnitude of enzyme concentrations.

Sensors array characterization

The array of photosensors is designed to allow the simultaneous measurement of 16 different luminescent reactions, occurring simultaneously in a spatially resolved configuration, thus leading to a system suitable for multiplex bioassays. For this purpose, it is necessary to ensure that all the photosensors uniformly respond to a given light signal, independently on their position on the array, and to verify absence of crosstalk phenomena among adjacent photosensors.

Inter-sensor reproducibility

First, inter-sensor reproducibility was assessed by depositing on each photodiode an aliquot of the same CL cocktail containing HRP at low (0.2 pg μL^{-1}) and high (2 pg μL^{-1}) levels. Signals were acquired simultaneously for all the photosensors, obtaining a maximum variability of the signal between photosensors of 3 %.

Crosstalk

The inter-site crosstalk was assessed by pouring HRP CL solutions at different concentrations in the highest investigated range (between 0.2 and 50 pg μL^{-1}) in one of the black PDMS wells and by comparing the signal of the selected site with that of the all neighboring sites. The crosstalk signal between photosensors results negligible being well below the noise level of the sensors, thus proving that the geometrical design of the array in terms of sensor size and spacing, combined with the use of black PDMS structure for sample confinement is correct making the device suitable for the simultaneous measurement of multiple analytes.

Model luminescent bioanalytical assays

Reported data show satisfactory performance of a-Si:H photosensors, as compared with state-of-the-art laboratory instrumentation. Indeed, despite reduced size and power consumption, as well as absence of photosensors cooling, they provided limits of detection that are only slightly higher than those obtained with reference instrumentation in the same conditions. In these experiments, a 4 s integration time was employed, however, if lower limits of detection are required, the use of longer signal integration times will increase signal-to-noise ratio, which grows with the square root of the signal integration time.

With such stated performance, the applicability of the integrated a-Si:H photosensor array to real bioanalytical assays was evaluated, by application of a model BL cytotoxicity assay and a CL total antioxidant capacity assay. In the latter, the possibility to follow the CL emission in real-time over a large number of consecutive acquisitions and conveniently store and eventually process the acquired data is crucial for assay performance.

Bioluminescence cytotoxicity assay

To prove applicability to cell-based bioassays, a model cytotoxicity assay was performed employing the microwell PDMS cartridge. For this purpose, HEK293 cells genetically modified to stably express Luc were treated with DMSO at different concentrations (in the range 2–50 %*v*/*v*) as a model toxic compound. The addition of DMSO to the cells suspension causes cell membrane disruption, leading to a reduction in cell metabolism and viability, thus lowering the BL signal.

The BL emission of the blank was set to 100 %, then BL emission of treated cells was normalized accordingly and plotted against DMSO concentration, as reported in Fig. 7. As expected, the toxic effect of DMSO resulted in a sharp decrease in the BL signal, and a half lethal concentration (LC50) of 13 % (*v*/*v*) DMSO was calculated as the DMSO concentration producing a 50 % reduction in light.

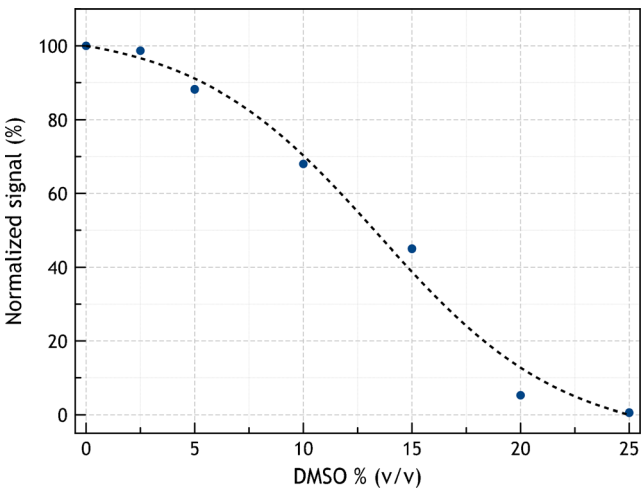

Fig. 7 Normalized cytotoxicity curve for DMSO, as measured employing a-Si:H photosensors

Chemiluminescence measurement of total antioxidant capacity

A CL assay for measuring total antioxidant capacity in biological samples was applied on the developed microcartidge with integrated photosensors array. The assay is based on the ability of antioxidants (i.e. compounds with a reduction potential lower than that of luminol) to quench the enhanced HRP-catalyzed luminol CL reaction [46]. As a consequence, CL emission is quenched as long as antioxidants are present in the mixture and it recovers as soon as all antioxidants are oxidized. The recovery time is employed to determine the total antioxidant capacity of a sample, as compared with the response of a standard antioxidant (in this work ascorbic acid). In this type of assay, the ability to simultaneously record in real-time the evolving CL reactions is fundamental as the analytical information is given by the time of the 50 % signal recovery.

Figure 8 (top) reports the evolving signals measured for the CL cocktail in the presence of different amounts of ascorbic acid. By plotting the time of 50 % signal recovery against ascorbic acid concentration, a linear calibration curve was obtained.

In parallel, two extracts from red grape juice were assayed, one obtained through extraction in water and one in ethanol. Preliminary experiments allowed establishing that the optimal dilution factor to obtain signal recovery within 10 min was 1:100 (*v*/*v*) and 1:500 (*v*/*v*) for the aqueous and the alcoholic extracts, respectively. As expected for samples containing a mixture of different antioxidant compounds, a smooth increase of the CL signal is observed (Fig. 8, bottom), as compared with sharp increase of the CL signal observed in the presence of the standard antioxidant ascorbic acid. The time of 50 % signal recovery of each sample interpolated on the calibration curve, which provided the total antioxidant capacity of the sample expressed as ascorbic acid equivalents, was: 14 mM for the ethanol extract and 3.5 mM for the aqueous extract, showing, as expected, a higher antioxidants extraction ability of alcoholic solutions with respect to aqueous ones.

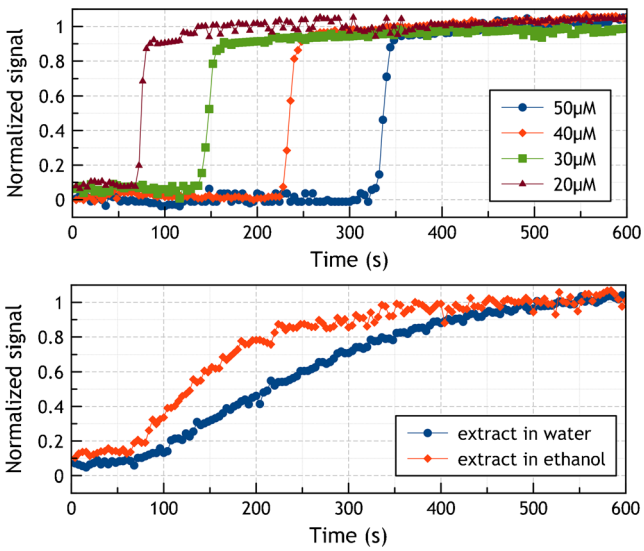

Fig. 8 Real-time monitoring of CL emission of the HRP/CL cocktail in the presence of ascorbic acid standard solutions (*upper panel*) or red grape juice extracts (*lower panel*). Signals have been normalized with respect to the CL signal measured at each time point for the blank (HRP/CL cocktail added of buffer instead of antioxidants)

Conclusions

In the present work, the performance of a new photosensors chip was evaluated in view of its application for the development of a BL and CL-based LOC device integrating the analytical detection system and the transduction into the chip.

The a-Si:H photosensors used in this work were deposited on a glass support and patterned in a 4×4 matrix in order to allow multiplex analyses. The opposite side of the support was coupled with a multiwell PDMS microcartridge in order to carry out the luminescence reactions in positions corresponding to the sensors, for optimal optical coupling. The a-Si:H photosensors are inexpensive to manufacture and they are amenable to fabrication in different sizes, from the hundreds of micrometers to tens of millimeters scale. For multiplex applications, they can be produced in arrays, in which the number of sensors is virtually limited only by the size of the glass substrate and their density by the crosstalk phenomena, which can be controlled by careful design of the array geometry [38].

When tested on BL and CL reactions catalyzed by enzymes, which are frequently employed in bioassays, the photosensors show low instrumental noise levels, a good inter-sensor reproducibility within the array, negligible crosstalk between adjacent sensors, and LOD values fairly well comparable with those obtained employing reference laboratory instrumentation. In particular, the limits of detection in the order of attomoles to femtomoles calculated for HRP, AP and firefly Luc enzyme labels and the linearity of response extending up to three orders of magnitude make the a-Si:H photosensors valuable candidates for analytical applications in BL and CL-based LOC devices.

The competitiveness of a-Si:H photosensor array with respect to cooled CCD detectors regards both device dimensions and costs, without a significant loss in detectability. It is important to note that, while the CCD results refer to thermally cooled device, the a-Si:H photosensor performances were achieved at room temperature (about 25 °C) showing that the proposed system is suitable for in-the-field applications. In addition, the digital memory occupancy of the measured data in the presented multiwell cartridge is significantly lower

than those of image-based systems, which positively affects not only the data storage but also the algorithm complexity and computing time for data analysis.

The multiwell cartridge with integrated photosensors might find application in the development of rapid homogeneous assays, while for heterogeneous assays, integration of the arrayed photosensors in a microfluidic device will be best suited and it is subject of currently ongoing work. We can state therefore that the proposed a-Si:H photosensor array, when integrated with microfluidic chips, provides compact, sensitive and potentially low-cost microdevices for BL- and CL-based bioassays with a wide range of possible applications for in-field and point-of-care bio-analyses.

Acknowledgments Financial support was provided by the Italian Ministry of Instruction, University and Research: PRIN 2009 project: prot. 2009MB4AYL "Integration of biosensing and nanotechnology for medical diagnostics with high analytical performance" and PRIN 2010 project: prot. 20108ZSRTR "ARTEMIDE (Autonomous Real Time Embedded Multi-analyte Integrated Detection Environment): a fully integrated lab-on-chip for early diagnosis of viral infections". Financial support was also provided by the Center for Life Nano Science@Sapienza, Istituto Italiano di Tecnologia (Viale Regina Elena 291, 00161 Rome, Italy).

References

1. Abgrall P, Gue A-M (2007) Lab-on-chip technologies: making a microfluidic network and coupling it into a complete microsystem—a review. J Micromech Microeng 17:R15–R49
2. Arora A, Simone G, Salieb-Beugelaar GB, Kim JT, Manz A (2010) Latest developments in micro total analysis systems. Anal Chem 82: 4830–4847
3. Costantini F, Nascetti A, Scipinotti R, Domenici F, Sennato S, Gazza L, Bordi F, Pogna N, Manetti C, Caputo D, de Cesare G (2014) On-chip detection of multiple serum antibodies against epitopes of celiac disease by an array of amorphous silicon sensors. RSC Adv 4:2073–2080
4. Seidel M, Niessner R (2008) Automated analytical microarrays: a critical review. Anal Bioanal Chem 391:1521–1544
5. Marquette CA, Corgier BP, Blum LJ (2012) Recent advances in multiplex immunoassays. Bioanalysis 4:927–936
6. Marquette CA, Blum LJ (2009) Chemiluminescent enzyme immunoassays: a review of bioanalytical applications. Bioanalysis 1:1259–1269
7. Roda A, Guardigli M, Pasini P, Mirasoli M, Michelini E, Musiani M (2005) Bio- and chemiluminescence imaging in analytical chemistry. Anal Chim Acta 541:25–36
8. Roda A, Pasini P, Guardigli M, Baraldini M, Musiani M, Mirasoli M (2000) Bio- and chemiluminescence in bioanalysis. Fresen J Anal Chem 366:752–759
9. Roda A, Guardigli M, Michelini E, Mirasoli M (2009) Bioluminescence in analytical chemistry and in vivo imaging. Trac-Trends Anal Chem 28:307–322
10. Mirasoli M, Guardigli M, Michelini E, Roda A (2014) Recent advancements in chemical luminescence-based lab-on-chip and microfluidic platforms for bioanalysis. J Pharm Biomed Anal 87: 36–52
11. Kricka LJ, Park JY (2011) Miniaturized analytical devices based on chemiluminescence, bioluminescence and electrochemiluminescence. In: Roda A (ed) Chemiluminescence and bioluminescence—past, present and future. RSC, Cambridge
12. Berthold F, Hennecke M, Wulf J (2011) Instrumentation for chemiluminescence and bioluminescence. In: Roda A (ed) Chemiluminescence and bioluminescence—past, present and future. RSC, Cambridge, pp 113–139
13. Roda A, Mirasoli M, Dolci LS, Buragina A, Bonvicini F, Simoni P, Guardigli M (2011) Portable device based on chemiluminescence lensless imaging for personalized diagnostics through multiplex bioanalysis. Anal Chem 83:3178–3185
14. Roda A, Cevenini L, Michelini E, Branchini BR (2011) A portable bioluminescence engineered cell-based biosensor for on-site applications. Biosens Bioelectron 26:3647–3653
15. Mirasoli M, Bonvicini F, Dolci LS, Zangheri M, Gallinella G, Roda A (2013) Portable chemiluminescence multiplex biosensor for quantitative detection of three B19 DNA genotypes. Anal Bioanal Chem 405:1139–1143
16. Kamei T, Toriello NM, Lagally ET, Blazej RG, Scherer JR, Street RA, Mathies RA (2005) Microfluidic genetic analysis with an integrated a-Si:H detector. Biomed Microdevices 7:147–152
17. Carlson DE (1977) Amorphous silicon solar cells. IEEE Trans Electr Dev 24:449–453
18. Ibaraki N (1994) a-Si TFT technologies for am-LCDs. Materials Research Society Symposium Proceedings, Cambridge Univ Press, 336:749–749
19. de Cesare G, Gavesi M, Palma F, Riccò B (2003) A novel a-si: H mechanical stress sensor. Thin Solid Films 427:191–195
20. Caputo D, de Cesare G, Nascetti A, Tucci M (2008) Detailed study of amorphous silicon ultraviolet sensor with chromium silicide window layer. IEEE Trans Electr Dev 55:452–456
21. Louro P, Fernandes M, Fantoni A, Lavareda G, Nunes de Carvalho C, Schwarz R, Vieira M (2006) An amorphous SIC/SI image photodetector with voltage-selectable spectral response. Thin Solid Films 511–512:167–171
22. Caputo D, de Cesare G, Nascetti A, Palma F, Petri M (1998) Infrared photodetection at room temperature using photocapacitance in amorphous silicon structures. Appl Phys Lett 72:1229–1231
23. Fixe F, Chu V, Prazeres D, Conde JP (2004) An on-chip photodetector for the quantification of DNA probes and targets in microarrays. Nucleic Acids Res 329:70–75
24. de Cesare G, Caputo D, Nascetti A, Guiducci C, Riccò B (2006) a-Si: H ultraviolet sensor for deoxyribonucleic acid analysis. Appl Phys Lett 88:083904–083906
25. Caputo D, de Cesare G, Nascetti A, Negri R (2006) Spectral tuned amorphous silicon p-i-n for DNA detection. J Non-Cryst Solids 352: 2004–2006
26. Caputo D, de Cesare G, Fanelli C, Nascetti A, Ricelli A, Scipinotti R (2012) Amorphous silicon photosensors for detection of Ochratoxin A in wine. IEEE Sens J 12:2674–2679
27. Novo P, Prazeres DMF, Chu V, Conde JP (2011) Microspot-based ELISA in microfluidics: chemiluminescence and colorimetry detection using integrated thin-film hydrogenated amorphous silicon photodiodes. Lab Chip 11:4063–4071
28. Novo P, Moulas G, Prazeres DMF, Chu V, Conde JP (2013) Detection of ochratoxin A in wine and beer by chemiluminescence-based ELISA in microfluidics with integrated photodiodes. Sensor Actuat B-Chem 176:232–240
29. Caputo D, de Cesare G, Dolci LS, Mirasoli M, Nascetti A, Roda A, Scipinotti R (2013) Microfluidic chip with integrated a-Si:H photodiodes for chemiluminescence-based bioassays. IEEE Sens J 13: 2595–2602
30. Caputo D, de Cesare G, Scipinotti R, Mirasoli M, Roda A, Zangheri M, Nascetti A (2014) Chemiluminescence-based micro-total-analysis system with amorphous silicon photodiodes. Lect Notes Electr Eng 268:207–211

31. Nascetti A, Truglio M, Valerio P, Caputo D, de Cesare G (2011) High dynamic range current-to-digital readout electronics for lab-on-chip applications. Proc 4th IEEE Int Work Adv Sensors Interfaces art. no. 6004691:77–81
32. Wieczorek H (1995) Effects of trapping in a-Si: H diodes. Solid State Phenom 44–46:957–972
33. Yang MH, Sun S, Kostov Y, Rasooly A (2010) Lab-on-a-chip for carbon nanotubes based immunoassay detection of Staphylococcal Enterotoxin B (SEB). Lab Chip 10:1011–1017
34. Oswald S, Karsunke X, Dietrich R, Martlbauer E, Niessner R, Knopp D (2013) Automated regenerable microarray-based immunoassay for rapid parallel quantification of mycotoxins in cereals. Anal Bioanal Chem 405:6405–6415
35. Heyries KA, Loughran MG, Hoffmann D, Homsy A, Blum LJ, Marquette CA (2008) Microfluidic biochip for chemiluminescent detection of allergen-specific antibodies. Biosens Bioelectron 23: 1812–1818
36. Szkola A, Campbell K, Elliott CT, Niessner R, Seidel M (2013) Automated, high performance, flow-through chemiluminescence microarray for the multiplexed detection of phycotoxins. Anal Chim Acta 787:211–218
37. Donhauser SC, Niessner R, Seidel M (2011) Sensitive quantification of Escherichia coil O157:H7, Salmonella enterica, and Campylobacter jejuni by combining stopped polymerase chain reaction with chemiluminescence flow-through DNA microarray analysis. Anal Chem 83:3153–3160
38. Pereira AT, Pimentel AC, Chu V, Prazeres DMF, Conde JP (2009) Chemiluminescence detection of horseradish peroxidase using an integrated amorphous silicon thin-film photosensor. IEEE Sens J 9: 1282–1290
39. Liu C-H, Chang Y-C, Norris TB, Zhong Z (2014) Graphene photodetectors with ultra-broadband and high responsivity at room temperature. Nat Nanotechnol 9:273–278
40. Wang X, Amatatongchai M, Nacapricha D, Hofmann O, de Mello JC, Bradley DDC, de Mello AJ (2009) Thin-film organic photodiodes for integrated on-chip chemiluminescence detection—application to antioxidant capacity screening. Sensor Actuat B-Chem 140:643–648
41. Matos Pires NM, Dong T, Hanke U, Hoivik N (2013) Integrated optical microfluidic biosensor using a polycarbazole photodetector for point-of-care detection of hormonal compounds. J Biomed Opt 18:097001
42. Adam W, Bronstein I, Edwards B, Engel T, Reinhardt D, Schneider FW, Trofimov AV, Vasil'ev RF (1996) Electron exchange luminescence of spiroadamantane-substituted dioxetanes triggered by alkaline phosphatase. Kinetics and elucidation of pH effects. J Am Chem Soc 118:10400–10407
43. Roda A, Pasini P, Musiani M, Girotti S, Baraldini M, Carrea G, Suozzi A (1996) Chemiluminescent low-light imaging of biospecific reactions on macro- and microsamples using a videocamera-based luminograph. Anal Chem 68:1073–1080
44. Easton PM, Simmonds AC, Rakishev A, Egorov AM, Candeias LP (1996) Quantitative model of the enhancement of peroxidase-induced luminol luminescence. J Am Chem Soc 118:6619–6624
45. Marzocchi E, Grilli S, Della Ciana L, Prodi L, Mirasoli M, Roda A (2008) Chemiluminescent detection systems of horseradish peroxidase employing nucleophilic acylation catalysts. Anal Biochem 377: 189–194
46. Saleh L, Plieth C (2010) Total low-molecular-weight antioxidants as summary parameter, quantified in biological samples by a chemiluminescence inhibition assay. Nat Protoc 5:1627–1634